Effect of Lysine-28 Side-Chain Acetylation on the Nanomechanical Behavior of Alzheimer Amyloid β25−35 Fibrils

Á. Karsai,[†] A. Nagy,[†] A. Kengyel,[†] Z. Mártonfalvi,[†] L. Grama,[†] B. Penke,[‡] and M. S. Z. Kellermayer*,[†]

Department of Biophysics, University of Pécs, Faculty of Medicine, Pécs, H-7624 Hungary, and Department of Medicinal Chemistry and Protein Research Group of the Hungarian Academy of Sciences, University of Szeged, Szeged, H-6720 Hungary

Received April 29, 2005

Amyloid fibrils are self-associating filamentous structures formed from the 39- to 42-residue-long amyloid β peptide (Aβ peptide). The deposition of Aβ fibrils is one of the most important factors in the pathogenesis of Alzheimer's disease. Aβ25−35 is a fibril-forming peptide that is thought to represent the biologically active, toxic form of the full-length Aβ peptide. We have recently shown that β sheets can be mechanically unzipped from the fibril surface with constant forces in a reversible transition, and the unzipping forces differ in fibrils composed of different peptides. In the present work, we explored the effect of ε-amino acetylation of the Lys28 residue on the magnitude of the unzipping force of Aβ25−35 fibrils. Although the gross structure of the Lys28-acetylated (Aβ25−35_K28Ac) and wild-type Aβ25−35 (Aβ25−35wt) fibrils were similar, as revealed by atomic force microscopy, the fundamental unzipping forces were significantly lower for Aβ25−35_K28Ac (20 ± 4 pN SD) than for Aβ25−35wt (42 ± 9 pN SD). Simulations based on a simple two-state model suggest that the decreased unzipping forces, caused most likely by steric constraints, are likely due to a destabilized zippered state of the fibril.

INTRODUCTION

Alzheimer's disease is a neurodegenerative disorder, among others, characterized by the deposition of insoluble filamentous aggregates called neuritic plaques.[1,2] The major component of neuritic plaques is the 39- to 43-residue-long amyloid β peptide (Aβ) that forms self-associating fibrillar structures possessing predominantly cross-β conformation.[3] The structure of Aβ has been difficult to explore with conventional methods because of the insolubility and aggregation of the peptide. Recent site-directed spin labeling[4] and solid-state NMR experiments[5,6] have formed the basis of a high-resolution model of the Aβ1−40 fibril. According to the model, β hairpins oriented perpendicularly to the fibril axis are assembled into β sheets that line up to form protofilaments. Aβ protofilaments then associate in parallel to form the 6- to 8-nm-wide Aβ fibrils.

The amyloid β25−35 peptide (Aβ25−35) is a fragment of a full-length Aβ comprising a stretch of residues from position 25 to 35. Aβ25−35 has been thought to be the biologically active fragment of Aβ, considering that it forms fibrils and retains the toxicity of the full-length peptide.[7] Therefore, Aβ25−35 is often chosen as a model system for structural and functional studies of Aβ.

Recently, we explored the mechanical properties of different Aβ fibrils using single-molecule manipulation techniques.[8] Single-molecule manipulation experiments provide unique insights into not only the structure and elasticity but also the mechanically driven transitions of molecular systems.[9−17] We found that filamentous entities most likely corresponding to β sheets can be unzipped from the fibril with constant forces in an equilibrium process, indicating that, during mechanical relaxation, the β sheets rapidly rebind to the fibril surface. The rapid, mechanical zipping-together of β sheets could be an important mechanism behind cooperative amyloid fibril formation. Importantly, we observed that the fundamental unzipping forces were different for Aβ1−40 and Aβ25−35, suggesting that the chemical nature of the peptide influences, most likely via side-chain interactions, the structural dynamics of the fibril.[8] We have suggested that the interaction of the Lys28 side chain of Aβ25−35 with its neighborhood may affect the structural dynamics of the fibril.[8] To explore the influence of residue side-chain properties on Aβ-fibril structural dynamics, in the present work, we studied the effect of Lys28 ε-amino modification on the nanomechanical properties of Aβ25−35. We find that the side-chain acetylation significantly reduces the fundamental unzipping force, but the process retains its reversible nature. Monte Carlo simulations suggest that the decrease in unzipping force is most likely caused by a decrease in the stability of the zippered state. The changes in the nanomechanical properties of Aβ25−35 evoked by Lys28 acetylation may be attributed to steric constraints imposed on the system by the added acetyl group.

MATERIALS AND METHODS

Samples. Amyloid peptides were prepared by solid-phase synthesis.[18] Aβ25−35 peptide contains amino acid residue numbers 25−35 of the β peptide (Figure 1a). The unmodified Aβ25−35 peptide is designated here as Aβ25−35wt, and

* Corresponding author. Tel.: +36−72/536271. Fax: +36−72/536261. E-mail: miklos.kellermayer.jr@aok.pte.hu.
[†] University of Pécs.
[‡] University of Szeged.

10.1021/ci0501701 CCC: $30.25
Published on Web 10/07/2005

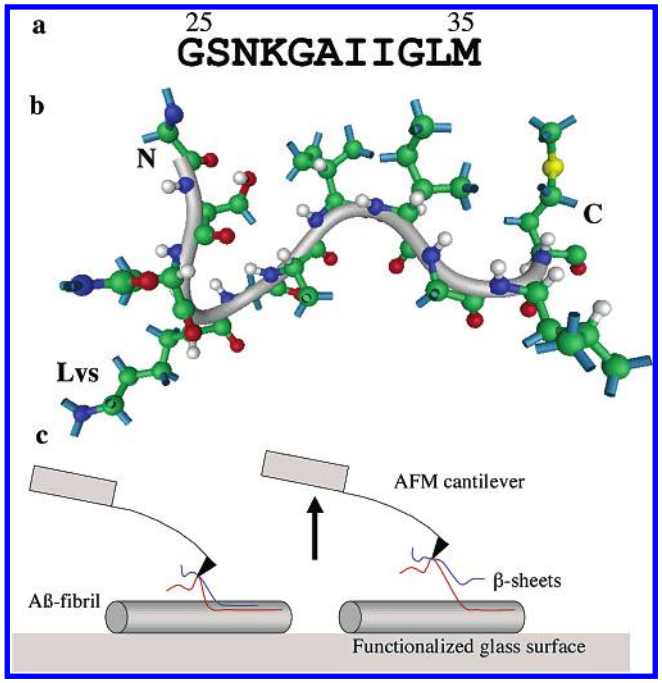

Figure 1. (a) Sequence of the Aβ25−35 peptide. (b) Structural model of the Aβ25−35 peptide in solution.[19] The Lys28 residue and the N and C termini of the peptide are indicated. The structural model was displayed using iMol software for Mac OSX. (c) Schematics of the experimental arrangement. Aβ25−35 fibrils were attached to silanized glass coverslip and manipulated with the tip of an AFM cantilever. By pulling the cantilever away from the fibril, β sheets were zipped from the surface.[8] In the schematic diagram, blue- and red-colored β sheets become completely unzipped from the fibril surface at different times during the experiment.

the Lys28-modified peptide is designated as Aβ25−35_K28Ac. The synthetic peptides contained an amide group at the C terminus. The solution structure of Aβ25−35wt, as determined recently,[19] is shown in Figure 1b. Fibrils were generated by dissolving the peptides in PBSA buffer (10 mM potassium phosphate, pH 7.4, 140 mM NaCl, 0.02% NaN_3) at a 0.5 mg/mL concentration. Aβ25−35 fibrils were grown in solution at room temperature for several days.

Surface Adsorption of Amyloid Fibrils. For atomic force microscopy (AFM) and molecular force spectroscopy measurements, fibrils were attached covalently to a silanized glass coverslip.[8] Briefly, coverslips were cleaned by sonication in acetone, followed by a rinsing with MilliQ water and drying them in a stream of N_2 gas. Precleaned coverslips were incubated in toluene vapor containing 2% (3-glycidyloxypropyl) trimethoxysilane (Fluka 50040) for 12 h at room temperature. A 50 μl sample containing Aβ fibrils (0.5 mg/mL concentration) preadjusted to pH 9 was pipetted onto the glass surface and incubated at room temperature for 30 min. Unbound fibrils were washed away by a rinsing with PBSA buffer.

Atomic Force Microscopy. Noncontact mode (AC mode) AFM images of amyloid fibrils bound to the silanized glass surface were acquired with an MFP3D (Asylum Research, Santa Barbara, CA) AFM instrument using silicon cantilevers (Olympus BioLever, typical resonance frequency ~30 kHz). 512 × 512 pixel images were collected at a typical scanning frequency of 0.6 Hz.

Single-Molecule Force Spectroscopy. Amyloid fibrils were stretched with AFM (Asylum Research MFP1D or MFP3D) by first pressing the cantilever (Olympus BioLever) tip against the surface, then pulling the cantilever away with a constant, preadjusted rate (Figure 1c). The typical stretch rate was 500 nm/s. Experiments were carried out under aqueous buffer conditions (PBSA buffer, pH 7.4). Stiffness was determined for each cantilever by using the thermal method.[20] Typical cantilever stiffness was ~30 pN/nm.

In Situ Force Spectroscopy. In situ force spectroscopy was carried out by, first, scanning (under aqueous buffer conditions) the glass-bound sample surface, then, pressing the cantilever tip to targeted surface locations identified on the image, and finally, rescanning the surface to test for the effect of the mechanical perturbations.[21] Soft (typical cantilever stiffness ~30 pN/nm), high-resonant-frequency (typical resonance frequency ~30 kHz) cantilevers (Olympus BioLever, B Lever) were used. Scanning was carried out in noncontact mode at high set-point values (0.8−1 V) to avoid the binding of the sample to the cantilever tip. To correct for drift, the same area was analyzed in several cycles of scanning and mechanical probing.

Data Analysis. Force step heights were obtained by measuring the distance between the average force values of consecutive plateaus (see Figure 2a).

Modeling and Simulation. Amyloid fibril unzipping was simulated with a simple elastically coupled two-state model[22,23] adapted to the mechanical unzipping of Aβ fibrils.[8] In the model, unzipping is a process in which a captured β sheet is gradually peeled off the fibril while the β strands of the β sheet are mechanically dissociated, one after the other, from the underlying surface. In the reverse zipping process, β strands of the β sheet rebind, one after the other, to the underlying fibril surface. The β-strand binding/dissociation (called, here, zipping/unzipping) activation kinetics are influenced by the mechanical load and the shape of the interaction potential holding the amyloid fibril together. In the simulation, the apparent contour length (L) of the captured β sheet is reduced by the presence of a set of bonds spaced 4.7 Å apart. As the chain is extended, force (f) was generated according to the wormlike chain (WLC) equation[24]

$$\frac{fA}{k_BT} = \frac{z}{L} + \frac{1}{4(1 - z/L)^2} - \frac{1}{4} \qquad (1)$$

where A is persistence length, k_BT is thermal energy, and z is the end-to-end distance. This entropic force is counterbalanced with the unzipping force. In each polling interval (dt), the probability of bond rupture (unzipping) at the given force (f) was calculated according to

$$P_u = \omega_0 \mathrm{dt}\, e^{-(E_{au} - f\Delta x_u)/k_BT} \qquad (2)$$

where ω_0 is the attempt frequency set by Brownian dynamics,[25] E_{au} is the activation energy of unzipping, and Δx_u is distance between the bound and transition states along the reaction coordinate. Similarly, in the same polling interval, the probability of binding (zipping) was calculated according to

$$P_z = \omega_0 \mathrm{dt}\, e^{-(E_{az} + f\Delta x_z)/k_BT} \qquad (3)$$

where E_{az} is the activation energy of zipping and Δx_z is the distance between the dissociated and transition states along

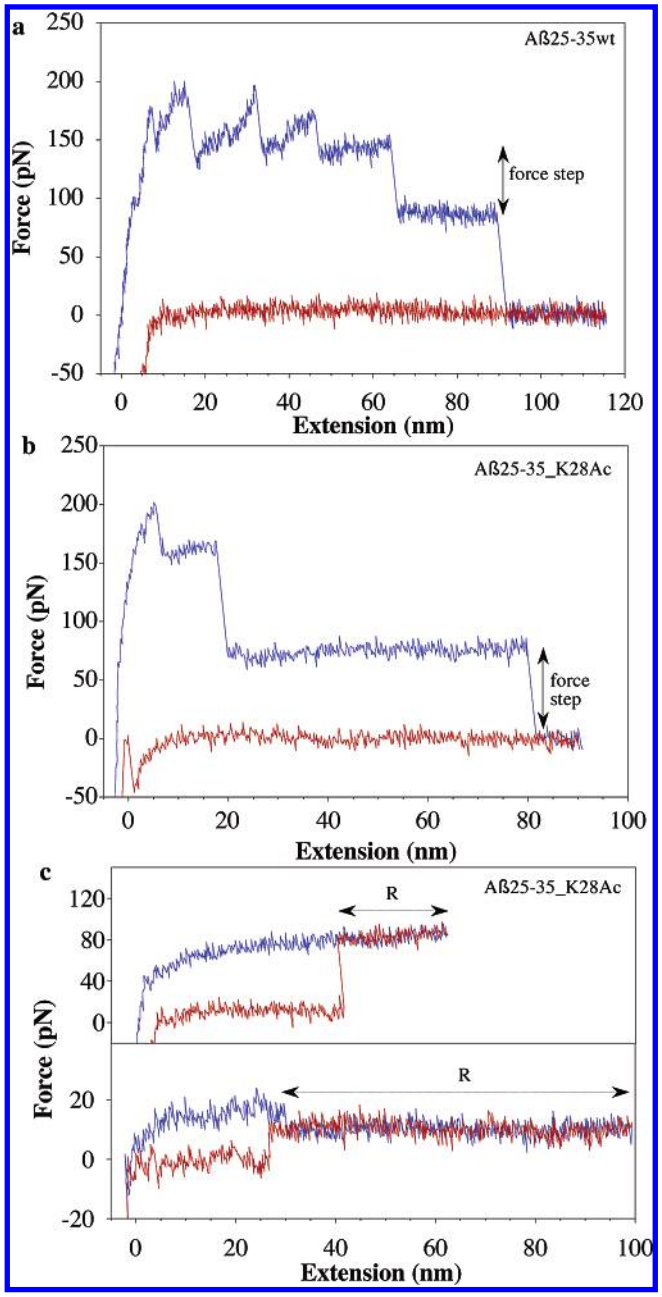

Figure 2. Force spectra of amyloid fibrils. Stretch data are shown in blue and release data in red. (a) Force spectrum of the Aβ25−35wt fibril. Lines with two arrowheads mark the concept of the force step analyzed in our study. (b) Force spectrum of the Aβ25−35_K28Ac fibril. (c) Examples of reversible force plateaus of Aβ25−35_K28Ac fibrils. Reversible regions (R) are indicated with dotted lines with two arrowheads.

the reaction coordinate. The unzipping or zipping processes were permitted or prohibited depending on a comparison of P with a number generated randomly between 0 and 1. Each bond rupture event incremented the apparent contour length with 4.7 Å and vice versa. The unzipping and zipping activation energies were adjusted so that their difference, which, in this simple two-state model, is equivalent to the free-energy change (ΔG) associated with the process, matched our experimental findings.

RESULTS AND DISCUSSION

Aβ25−35 fibrils were mechanically manipulated in this work by using AFM. We compared the nanomechanical properties of "wild-type" Aβ25−35 fibrils (Aβ25−35wt), the solution structure of which is shown in Figure 1b,[19] with those of Lys28 ϵ-amino-acetylated Aβ25−35 fibrils (Aβ25−35_K28Ac).

Morphology of Aβ25−35 Fibrils. AFM images of Aβ25−35 fibrils adsorbed to the silanized glass surface are shown in Figure 3a and b. The topographical height of the fibrils, which reflects their diameter, was approximately 8 nm for both Aβ25−35wt and Aβ25−35_K28Ac. Thus, upon first approximation, the overall structure of the two fibril types appear similar.

Surface-adsorbed amyloid fibrils were mechanically manipulated by pressing the AFM cantilever into the fibril, then pulling the cantilever away from the fibril surface at a constant rate (Figure 1c). The effect of mechanical perturbation on the overall fibril structure was investigated with in situ force spectroscopy (Figure 3c and d). In these experiments, the sample surface was scanned prior to (Figure 3c) and following (Figure 3d) the mechanical perturbations. According to our measurements, the mechanical perturbations did not result in structural changes resolvable with surface scanning, which suggests that the dimensions of the subfibrillar components unzipped from the fibril surface fall below the resolution of the technique. Considering that the gross structure of the fibrils was unaffected and no resolvable material loss was accrued, it is unlikely that entire protofilaments within the fibrils were perturbed. Rather, the unzipped subfibrillar components are β sheets, which also supports our previous observations.[8]

Force Spectroscopy of Aβ25−35 fibrils. The force spectra of the amyloid fibrils displayed multiple force steps (Figure 2).[8] The force steps arise as the hierarchical combination and superimposition of several force plateaus. During the force plateau, a constant force level is maintained during extension of the molecular system. A force plateau ends with an abrupt, stepwise decrease in force. The force plateaus correspond to gradual unzipping of the β sheets from the amyloid fibril surface.[8] Force remains constant during the process because, at each time point during extension, only a single set of bonds is loaded and broken mechanically. The height of the plateau is related to the energy of the bond(s) holding the β sheets associated to the fibril surface, provided that the system is in thermodynamic equilibrium. If several β sheets are grabbed and unzipped at the same time, then the height of the force plateau increases proportionally. Thus, the plateau height also reflects the number of β sheets unzipped from the fibril surface, which can be calculated on the basis of the single β-sheet unzipping force (fundamental unzipping force, see below). The abrupt force drop at the end of the plateau corresponds to the complete dissociation of the β sheet from the fibril surface.[8] Such a complete dissociation may occur either because the β sheet is mechanically ruptured or because the end of a discontinuous β sheet is reached. Multiple force steps arise because of the simultaneous unzipping of several β sheets that dissociate from the fibril at different times. The gradual mechanical dissociation of the β sheets results in subsequent steps that form force staircases. Although the overall appearance of the force spectra was similar for Aβ25−35wt and Aβ25−35_K28Ac, quantitative differences were measured (see below).

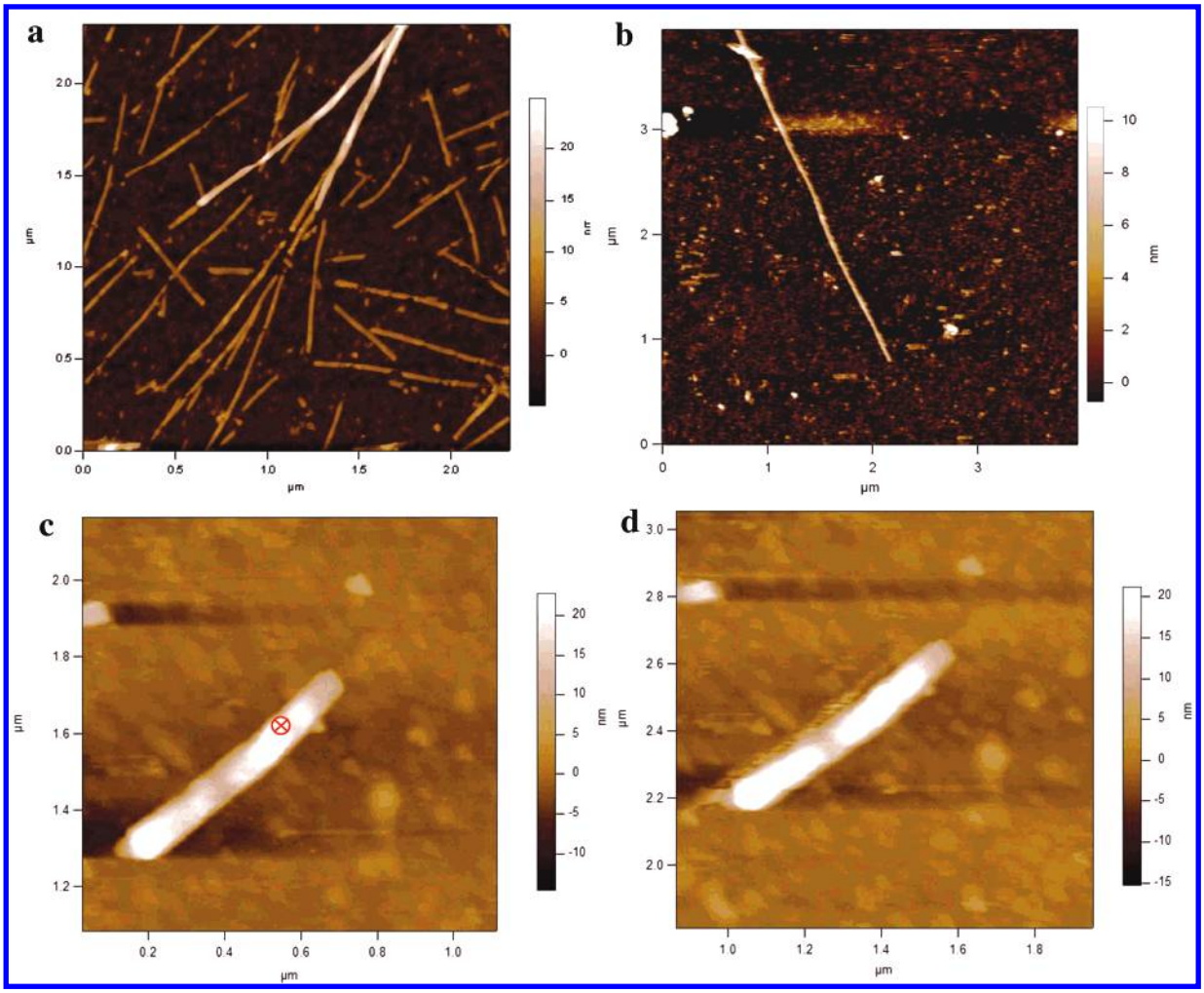

Figure 3. Scanning AFM images of amyloid fibrils. (a) AFM image of wild-type Aβ25−35 fibrils (Aβ25−35wt). (b) AFM image of Lys28-acetylated Aβ25−35 fibrils (Aβ25−35_K28Ac). (c) AFM image of an Aβ25−35_K28Ac fibril prior to mechanical manipulation. The red crosshair marks the location of the mechanical manipulation. (d) AFM image of the same Aβ25−35_K28Ac fibril following mechanical manipulation.

The observed force plateaus were reversible. That is, if the molecular system was allowed to contract prior to reaching the end of a force plateau, then the forces recorded during the retraction phase exactly coincided with those recorded during the stretch. Examples of reversible force plateaus in Aβ25−35_K28Ac are shown in Figure 2c. In these data, a force step occurs in the release trace, which is most likely caused by β-sheet rupture during the zipping process. The reversibility of the force plateau indicates that the molecular system is in thermodynamic equilibrium at each point of the extension.[14] Therefore, the free-energy change (ΔG) associated with the binding/dissociation of a β strand during zipping/unzipping can be calculated by integrating the area below the force plateau across a distance that corresponds to the β-strand spacing (4.7 Å),[3] provided that the unzipping force of a single β sheet is known.

Plateau Force Statistics. From the force-step heights, histograms were constructed. The force-step histograms displayed a multimodal distribution for both Aβ25−35wt and Aβ25−35_K28Ac (Figure 4). The histogram peaks appeared at forces that are integer multiples of a fundamental force. The peaks, therefore, correspond to forces necessary to unzip integer multiples of β sheets, and the fundamental unzipping force, identified as the lowest-force histogram peak, corresponds to the unzipping force of a single β sheet. The fundamental unzipping forces were 42 pN (±9 SD, $n = 199$) and 20 pN (±4 pN SD, $n = 71$) for Aβ25−35wt and Aβ25−35_K28Ac, respectively. Thus, significantly lower forces are required to unzip β sheets formed of the lysine28-acetylated Aβ25−35 peptide than those formed of the wild type. Presumably, acetylation weakens the interactions of the peptide and, therefore, the β sheet, with its structural neighborhood. One possibility is that the weakening is caused by the abolishment of the positive charge of the Lys28 ϵ-amino group by acetylation. The electrostatic interaction between the Lys28 ϵ-amino group and the C terminus of a neighboring peptide may stabilize the Aβ25−35 fibril.[8] Lys28 acetylation may, therefore, abolish the electrostatic stabilization. We exclude this possibility, however, because the synthetic peptides used herein contained an amide group at their carboxy terminus, which does not form attractive electrostatic interactions with the ϵ-amino group of Lys28. Rather, it is possible that the steric constraints imposed by the added acetyl group may weaken the intrafibrillar interaction of the peptides. In addition, the altered hydrogen-bonding system of the acetylated peptide may also weaken its interactions.

On the basis of the fundamental unzipping forces, it is possible to calculate the ΔG associated with β-strand binding/dissociation. Considering a β-strand spacing of 4.7 Å,[3] ΔG

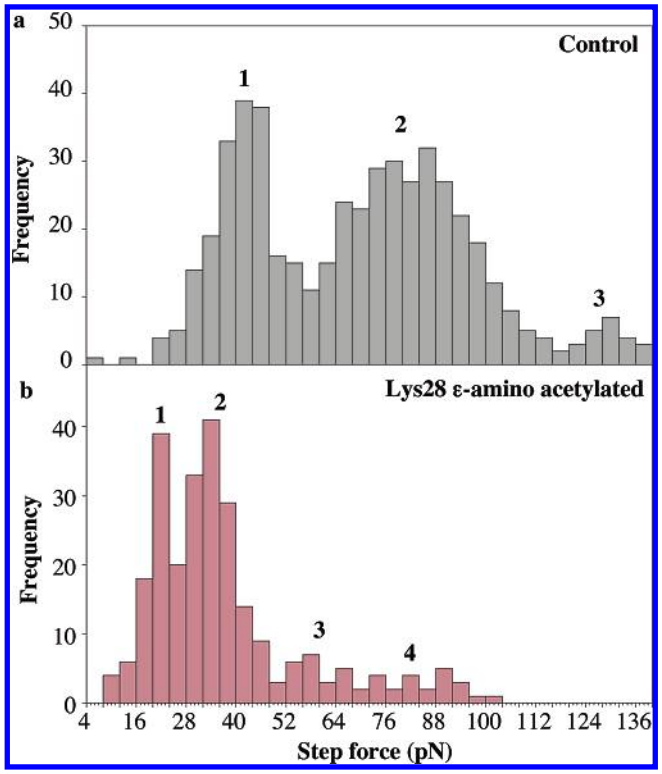

Figure 4. Step force statistics of Aβ25−35wt (a) and Aβ25−35_K28Ac (b). The numbers above the histogram peaks indicate the number of β sheets unzipped.

is 1.97 × 10^{-20} J and 9.4 × 10^{-21} J for single β strands of Aβ25−35wt and Aβ25−35_K28Ac, respectively, which corresponds to 11.82 and 5.64 kJ/mol, respectively.

Model and Simulation of Aβ-Fibril Nanomechanical Behavior. We modeled the force-driven Aβ-fibril zipping/unzipping process by using a simple two-state model.[8] The two states, which are separated by an activation energy barrier, are the zippered (or associated) and the unzipped (or dissociated) states. Mechanical force tilts the energy landscape of the system (Figure 5a),[26,27] so that the activation barrier is altered: unzipping is facilitated, while zipping is inhibited. Δ*G*, which is the difference between the free energies of the zippered and unzipped states and, within the two-state model, corresponds to the difference between the unzipping and zipping activation energies, is reduced in the case of Aβ25−35_K28Ac relative to that of Aβ25−35wt. The reduction of Δ*G* may occur as a result of an increase in the free energy of the zippered state, which corresponds to the destabilization of the zippered state. Figure 5a illustrates this scenario. Figure 5b shows the simulation results for a bundle of three β sheets zipped from the fibril surface, where the parameters were chosen according to the scenario above. The simulation recovered the essential features of our observations, including reversibility seen in the force curves (Figure 5b, inset). Simulation results indicated that the observed reduction in Δ*G* is explained by a destabilized zippered state. Possibly, the sterical constraints imposed on the system by side-chain acetylation may structurally destabilize the fibril.

CONCLUSIONS

In the present work, we manipulated amyloid fibrils formed from wild-type and Lys28-acetylated Aβ25−25 peptides. Although both fibril types displayed similar overall morphologies, we found differences in the magnitude of their nanomechanical behavior. Force plateaus and staircases were observed for both fibril types, which correspond to the unzipping of β sheets from the fibril surface. β sheets were unzipped from the fibril surface in a thermodynamically reversible transition. The force necessary to unzip individual β sheets, and hence the free-energy change of the transition, was decreased in the case of the Lys28-acetylated form. Monte Carlo simulations suggest that the changes are most plausibly explained by a destabilization of the zippered state, which is likely evoked by steric constraints imposed on the fibril by the added acetyl group. The nanomechanical fingerprinting used herein is, thus, a sensitive assay to monitor changes in the structural dynamics of amyloid fibrils.

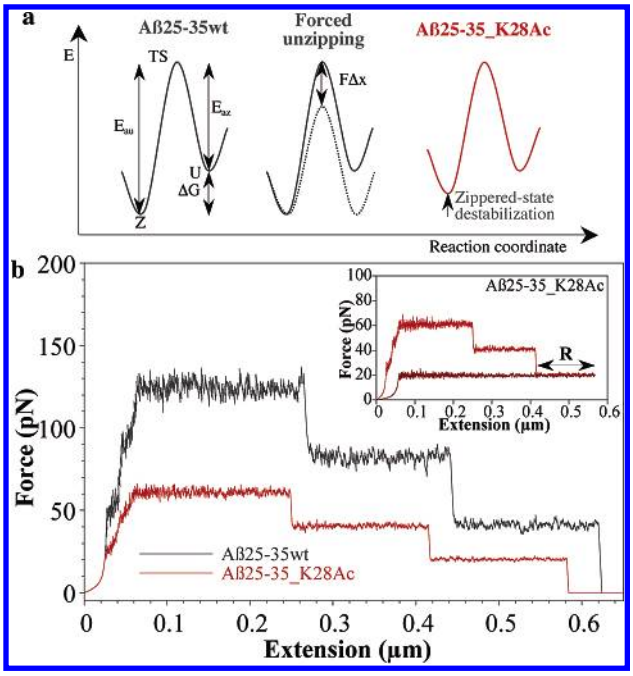

Figure 5. (a) Schematics of the unzipping energy landscape in terms of free energy along the unzipping reaction coordinate. Z is the zippered, U is the unzipped, and TS is the transition state. Δ*G* is the free-energy change associated with the unzipping/zipping transition and E_{au} and E_{az} are the unzipping and zipping activation energies, respectively. Mechanical force (*F*) tilts the energy landscape depending on the invested mechanical energy (*F*Δ*x*), where Δ*x* is a characteristic distance along the reaction coordinate between the zippered and transition states. The decrease in Δ*G* in the case of Aβ25−35_K28Ac may be evoked by the destabilization of the zippered state (red line, upward arrow). (b) Simulated mechanical response of Aβ25−35 fibrils in terms of force versus extension curves for a bundle of three β sheets unzipped from the fibril surface. Black and red lines mark the results for Aβ25−35wt and Aβ24−35_K28Ac, respectively. Inset: Test of reversibility, in which the simulated fibril was allowed to retract prior to the complete dissociation of the third β sheet. The coincidence of the stretch and relaxation data (R) indicates reversibility and, therefore, thermodynamic equilibrium. Relevant simulation parameters were Δx_u, 0.2 nm; Δx_z, 0.3 nm; E_{az}, 5 × 10^{-20} J. E_{au} was 7 × 10^{-20} and 6 × 10^{-20} for Aβ25−35wt and Aβ25−35_K28Ac, respectively.

ACKNOWLEDGMENT

This work was supported by grants from the Hungarian Science Foundation (OTKA T049591), Hungarian Ministry of Education (OM-110/2002), Hungarian Ministry of Health (ETT-440/2003), and the South Trans-Danubian Cooperative

Research Center. M.S.Z.K. is a Howard Hughes Medical Institute International Research Scholar.

REFERENCES AND NOTES

(1) Mattson, M. P. Pathways towards and away from Alzheimer's disease. *Nature* **2004**, *430* (7000), 631−9.
(2) Selkoe, D. J. Images in neuroscience. Alzheimer's disease: from genes to pathogenesis. *Am. J. Psychiatry* **1997**, *154* (9), 1198.
(3) Serpell, L. C. Alzheimer's amyloid fibrils: structure and assembly. *Biochim. Biophys. Acta* **2000**, *1502* (1), 16−30.
(4) Torok, M.; Milton, S.; Kayed, R.; Wu, P.; McIntire, T.; Glabe, C. G.; Langen, R. Structural and dynamic features of Alzheimer's Abeta peptide in amyloid fibrils studied by site-directed spin labeling. *J. Biol. Chem.* **2002**, *277* (43), 40810−5.
(5) Petkova, A. T.; Ishii, Y.; Balbach, J. J.; Antzutkin, O. N.; Leapman, R. D.; Delaglio, F.; Tycko, R. A structural model for Alzheimer's β-amyloid fibrils based on experimental constraints from solid-state NMR. *Proc. Natl. Acad. Sci. U.S.A.* **2002**, *99* (26), 16742−16747.
(6) Tycko, R. Progress towards a molecular-level understanding of amyloid fibrils. *Curr. Opin. Struct. Biol.* **2004**, *14*, 96−103.
(7) Pike, C. J.; Walencewicz-Wasserman, A. J.; Kosmoski, J.; Cribbs, D. H.; Glabe, C. G.; Cotman, C. W. Structure−activity analyses of beta-amyloid peptides: contributions of the beta 25−35 region to aggregation and neurotoxicity. *J. Neurochem.* **1995**, *64* (1), 253−65.
(8) Kellermayer, M. S.; Grama, L.; Karsai, A.; Nagy, A.; Kahn, A.; Datki, Z. L.; Penke, B. Reversible mechanical unzipping of amyloid beta-fibrils. *J. Biol. Chem.* **2005**, *280* (9), 8464−70.
(9) Brockwell, D. J.; Paci, E.; Zinober, R. C.; Beddard, G. S.; Olmsted, P. D.; Smith, D. A.; Perham, R. N.; Radford, S. E. Pulling geometry defines the mechanical resistance of a beta-sheet protein. *Nat. Struct. Biol.* **2003**, *10* (9), 731−7.
(10) Carrion-Vazquez, M.; Li, H.; Lu, H.; Marszalek, P. E.; Oberhauser, A. F.; Fernandez, J. M. The mechanical stability of ubiquitin is linkage dependent. *Nat. Struct. Biol.* **2003**, *10* (9), 738−43.
(11) Fisher, T. E.; Marszalek, P. E.; Fernandez, J. M. Stretching single molecules into novel conformations using the atomic force microscope. *Nat. Struct. Biol.* **2000**, *7* (9), 719−24.
(12) Fisher, T. E.; Oberhauser, A. F.; Carrion-Vazquez, M.; Marszalek, P. E.; Fernandez, J. M. The study of protein mechanics with the atomic force microscope. *Trends Biochem. Sci.* **1999**, *24* (10), 379−84.
(13) Kellermayer, M. S. Z.; Smith, S. B.; Granzier, H. L.; Bustamante, C. Folding-unfolding transitions in single titin molecules characterized with laser tweezers. *Science* **1997**, *276* (5315), 1112−6.
(14) Liphardt, J.; Onoa, B.; Smith, S. B.; Tinoco, I. J.; Bustamante, C. Reversible unfolding of single RNA molecules by mechanical force. *Science* **2001**, *292* (5517), 733−7.
(15) Rief, M.; Gautel, M.; Oesterhelt, F.; Fernandez, J. M.; Gaub, H. E. Reversible unfolding of individual titin immunoglobulin domains by AFM. *Science* **1997**, *276* (5315), 1109−1112.
(16) Smith, S. B.; Cui, Y.; Bustamante, C. Overstretching B-DNA: the elastic response of individual double-stranded and single-stranded DNA molecules. *Science* **1996**, *271* (5250), 795−9.
(17) Tskhovrebova, L.; Trinick, J.; Sleep, J. A.; Simmons, R. M. Elasticity and unfolding of single molecules of the giant muscle protein titin. *Nature* **1997**, *387* (6630), 308−12.
(18) Palotás, A.; Kálmán, J.; Palotás, M.; Juhász, A.; Janka, Z.; Penke, B. β-Amyloid-induced increase in the resting intracellular calcium concentration gives support to tell Alzheimer lymphocytes from control ones. *Brain Res. Bull.* **2002**, *58* (2), 203−205.
(19) D'Ursi, A. M.; Armenante, M. R.; Guerrini, R.; Salvadori, S.; Sorrentino, G.; Picone, D. Solution structure of amyloid beta-peptide (25−35) in different media. *J. Med. Chem.* **2004**, *47* (17), 4231−8.
(20) Hutter, J. L.; Bechhoefer, J. Calibration of atomic-force microscope tips. *Rev. Sci. Instrum.* **1993**, *64* (7), 1868−1873.
(21) Oesterhelt, F.; Oesterhelt, D.; Pfeiffer, M.; Engel, A.; Gaub, H. E.; Muller, D. J. Unfolding pathways of individual bacteriorhodopsins. *Science* **2000**, *288* (5463), 143−6.
(22) Kellermayer, M. S.; Bustamante, C.; Granzier, H. L. Mechanics and structure of titin oligomers explored with atomic force microscopy. *Biochim. Biophys. Acta* **2003**, *1604* (2), 105−14.
(23) Rief, M.; Fernandez, J. M.; Gaub, H. E. Elastically coupled two-level systems as a model for biopolymer extensibility. *Phys. Rev. Lett.* **1998**, *81* (21), 4764−4767.
(24) Bustamante, C. J.; Marko, J. F.; Siggia, E. D.; Smith, S. B. Entropic elasticity of λ-phage DNA. *Science* **1994**, *265*, 1599−1600.
(25) Bell, G. I. Models for the specific adhesion of cells to cells. *Science* **1978**, *200* (4342), 618−27.
(26) Evans, E.; Ritchie, K. Dynamic strength of molecular adhesion bonds. *Biophys. J.* **1997**, *72* (4), 1541−55.
(27) Evans, E.; Ritchie, K. Strength of a weak bond connecting flexible polymer chains. *Biophys. J.* **1999**, *76* (5), 2439−47.

CI0501701